

Chance Constrained Optimal Power Flow with Primary Frequency Response

Michael Chertkov
 Center for Nonlinear Studies
 Los Alamos National Laboratory
 Los Alamos, NM 87545
 chertkov@lanl.gov

Yury Dvorkin
 Dep. of Electrical & Computer Engineering
 Tandon School of Engineering
 New York University
 New York, NY 11201
 dvorkin@nyu.edu

Abstract—Primary frequency response is provided by synchronized generators through their speed-droop governor characteristic in response to instant frequency deviations that exceed a certain threshold, also known as the governor dead zone. This dead zone makes the speed-droop governor characteristic nonlinear and makes affine control policies that are often used for modeling the primary frequency response inaccurate.

This paper presents an optimal power flow (OPF) formulation that explicitly models i) the primary frequency response constraints using a nonlinear speed-droop governor characteristic and ii) chance constraints on power outputs of conventional generators and line flows imposed by the uncertainty of renewable generation resources. The proposed chance constrained OPF (CCOPF) formulation with primary frequency response constraints is evaluated and compared to the standard CCOPF formulation on a modification of the 118-bus IEEE Reliability Test System.

I. INTRODUCTION

As a result of policy initiatives and incentives, renewable generation resources have already exceeded 10% penetration levels, in terms of annual electricity produced, in some interconnections; even higher targets are expected to be reached in the forthcoming years [1]. Integrating renewable generation resources increases reserve requirements needed to deal with their uncertainty and variability and, at the same time, tends to replace conventional generation resources that are most suitable for the efficient reserve provision, [2]. Among these reserve requirements, the ability to provide sufficient *primary frequency response*, i.e. the automatic governor-operated response of synchronized generators intended to compensate a sudden power mismatch based on local frequency measurements, is the least studied [3]. The impacts of renewable generation resources on the secondary and tertiary reserve requirements are reviewed in [4], [5].

Data-driven studies in [6] and [7] manifestly reveal that the primary frequency response in major US interconnections has drastically reduced over the past decades and attribute this effect to increased penetrations of renewable generation resources. Primary frequency response constraints are modeled in [8] and [9]. These studies consider a nonlinear speed-droop governor characteristic with an intentional dead zone that makes it possible to preserve the primary frequency response for reacting to relatively large frequency deviations caused by sudden generation and demand failures [10].

However, the formulations in [8] and [9] ignore transmission constraints and the uncertainty of renewable generation resources that may lead to overload and capacity scarcity events when the primary frequency response is deployed.

To deal with the stochastic nature of renewable generation resources and their impacts on the secondary and tertiary reserve requirements, the standard optimal power flow (OPF) formulations have been enhanced using chance constrained programming [11], scenario-based stochastic programming [12] and robust optimization [13]. The formulation in [11] postulates the uncertainty and variability of wind power generation resources follow a given Gaussian distribution that makes it possible to convert the Chance Constrained OPF (CCOPF) into a second-order cone program, which is then solved using a cutting-plane-based procedure. Relative to [11], the formulation in [12] is more computationally demanding since it requires computationally expensive scenario sampling, [14]. Unlike [11] and [12], the formulation in [13] disregards the likelihood of individual scenarios within a given uncertainty range and tends to yield overly conservative solutions. Based on the CCOPF formulation in [11], several extensions have been developed. Reference [15] implements a distributionally robust CCOPF formulation that internalizes parameter uncertainty on the Gaussian distribution characterizing wind power forecast errors as explained in [16]. In [17], the CCOPF formulation is extended to accommodate corrective control actions. The formulation in [18] describes the CCOPF formulation that uses wind curtailments for self-reserve to reduce the secondary and tertiary reserve provision by conventional generation resources. In [19], the chance constraints are modified to selectively treat large and small wind power perturbations using weighting functions. Notably, the convexity of the original formulation in [11] is preserved in [15], [17]–[19].

The formulations in [11], [15], [17]–[19] have been proven to reliably and cost-efficiently deal with the uncertainty and variability imposed by renewable generation resources at a computational acceptable cost, even for realistically large networks [11], [15]. However, these formulations neglect to account for nonlinear primary frequency response policies, i.e. the dead zone of the speed-droop governor characteristic. From the reliability perspective, this may result in

the inability to timely arrest a frequency decay caused by credible contingencies, [6], [10], [20]. Furthermore, ignoring nonlinear primary frequency response policies may lead to suboptimal dispatch decisions and cause unnecessary out-of-market corrections that would eventually increase the overall operating cost, [21]. This paper proposes a CCOPF formulation with a nonlinear primary frequency response policy that seeks the least-cost primary frequency response provision among available conventional generation resources. The main contributions of this paper are as follows:

- 1) The proposed CCOPF-PFR formulation enhances the CCOPF formulation in [11] by explicitly considering primary frequency response constraints of conventional generators.
- 2) As in [8] and [9], the primary frequency response is modeled using a nonlinear speed-droop governor characteristic with an intentional dead zone, i.e. the primary frequency response does not react to frequency fluctuations below a given threshold.
- 3) The weighted chance constraints from [19] are used to reformulate the proposed CCOPF-PFR formulation into a convex program that can be solved using off-the-shelf solvers. The CCOPF-PFR and CCOPF formulations are compared using a modification of the 118-bus IEEE Reliability Test System [22].

The rest of this paper is organized as follows. Section II describes the proposed CCOPF-PFR formulation based on the standard CCOPF formulation in [11]. Section III describes the proposed solution technique. Section IV numerically compares the CCOPF-PFR and CCOPF formulations. Section V concludes the paper.

II. CCOPF-PFR FORMULATION

This section describes the CCOPF-PFR formulation in steps. First, Section II-A describes the CCOPF formulation from [11]. Next, a generic affine frequency control policy is reviewed in Section II-B. This affine policy is then modified in Section II-C to accommodate a given dead zone. Section II-D applies the weighted chance constraints from [19] and states the final CCOPF-PFR formulation.

A. Standard CCOPF

Using dc power flow assumptions, the following deterministic OPF can be formulated:

$$\min_{p_g, \phi, \theta} \sum_{i \in \mathcal{V}_g} C_i(p_i) \quad (1)$$

s. t.

$$\sum_{i \in \mathcal{V}} p_i = 0 \quad (2)$$

$$\forall i \in \mathcal{V}_g : p_i \in [\underline{p}_i, \bar{p}_i] \quad (3)$$

$$\forall i \in \mathcal{V} : p_i = \sum_{j: \{i, j\} \in \mathcal{E}} \phi_{ij} \quad (4)$$

$$\forall \{i, j\} \in \mathcal{E} : \phi_{ij} = \beta_{ij}(\theta_i - \theta_j) \quad (5)$$

$$\phi_{ij} \in [-\bar{\phi}_{ij}, \bar{\phi}_{ij}] \quad (6)$$

Eq. (1)-(6) are formulated for the transmission system described by undirected graph $\mathcal{G} = (\mathcal{V}, \mathcal{E})$, where \mathcal{V} and \mathcal{E} denote the sets of nodes (buses) and edges (transmission lines). The set of nodes consists of subsets of nodes with conventional generators (\mathcal{V}_g), loads (\mathcal{V}_l) and wind farms (\mathcal{V}_w), i.e. $\mathcal{V} = \mathcal{V}_g \cup \mathcal{V}_l \cup \mathcal{V}_w$. This optimization is performed over the vectors of decision variables on i) the power output of conventional generators $p_g = (p_i | i \in \mathcal{V}_g)$, ii) active power flows in transmission lines $\phi = (\phi_{ij} = -\phi_{ji} | \{i, j\} \in \mathcal{E})$ and iii) voltage angles $\theta = (\theta_i | i \in \mathcal{V})$. The input parameters include the minimum (\underline{p}_i) and maximum (\bar{p}_i) limits on the power output of conventional generators, vector of nodal loads ($p_l = (p_i | i \in \mathcal{V}_l)$), vector of wind power injections ($p_w = \rho = (\rho_i | i \in \mathcal{V}_w)$), as well as the line impedances ($\beta_{ij}, \forall \{i, j\} \in \mathcal{E}$) and power flow limits ($\bar{\phi}_{ij}, \forall \{i, j\} \in \mathcal{E}$) of transmission lines. Eq. (1) minimizes the total operating cost using a convex, quadratic cost function of each conventional generator, $C_i(\cdot)$. The system-wide power balance is enforced in Eq. (2). Eq. (3) limits the power output of conventional generators. The nodal power balance is enforced in Eq. (4) using the line flows computed in Eq. (5) based on dc power flow assumptions. Eq.(6) limits the line flows.

Eq. (1)-(6) seeks the least-cost solution assuming fixed power outputs of wind farms. In fact, these outputs are likely to vary due to the inherent wind speed uncertainty and variability [16] that can be accounted for by using a chance constrained framework, [11], [15]:

$$\min_{p_g^{(0)}, \theta, \rho} \sum_{i \in \mathcal{V}_g} \mathbb{E}_\rho [C_i(p_i)] \quad (7)$$

s. t.

$$\forall i \in \mathcal{V}_g : \text{Prob}_\rho [p_i \leq \underline{p}_i] \leq \varepsilon_i^\downarrow \quad (8)$$

$$\text{Prob}_\rho [p_i \geq \bar{p}_i] \leq \varepsilon_i^\uparrow \quad (9)$$

$$\forall \{i, j\} \in \mathcal{E} : \text{Prob}_\rho [\phi_{ij} \leq -\underline{\phi}_{ij}] \leq \varepsilon_{ij}^\downarrow \quad (10)$$

$$\text{Prob}_\rho [\phi_{ij} \geq \bar{\phi}_{ij}] \leq \varepsilon_{ij}^\uparrow. \quad (11)$$

where $\rho = p_w$ is the exogenous statistics of wind power outputs that is assumed to be Gaussian and described as:

$$\forall i \in \mathcal{V}_w : \mathbb{E} [\rho_i] = \bar{\rho}_i, \quad (12)$$

$$\mathbb{E} [(\rho_i - \bar{\rho}_i)^2] = R_i, \quad (13)$$

where $\bar{\rho}_i$ and R_i are the mean and covariance. The optimization in Eq. (7)-(11) assumes that p_l remains fixed, as in Eq. (1)-(6), while p_g depends on ρ . This dependency makes it possible for conventional generators to deviate from their original set points, $p_g^{(0)}$, to follow random wind power outputs according to a given control policy. This policy can be affine or nonlinear as discussed in Section II-B and Section II-C, respectively. Eq. (8) and (11) are chance constrained equivalents of Eq. (3) and (6), respectively. Parameters $\varepsilon_i^\uparrow, \varepsilon_i^\downarrow, \varepsilon_{ij}^\uparrow, \varepsilon_{ij}^\downarrow$ can be interpreted as proxies for the fraction of time (probability) when a constraint violation can be tolerated, [11]. Relative to [11], [15], the optimization in Eq. (7)–(11) has several simplifications made for the sake of clarity. First, it assumes compulsory participation of conventional

generators in the frequency control provision. Second, it ignores parameter uncertainty on the probability distribution characterizing wind power generation and correlation between distribution parameters at different nodes.

B. Affine Frequency Control

The balanced system is characterized by $\sum_{i \in \mathcal{V}} p_i^{(0)} = 0$. Under random fluctuations of wind power outputs given by $\sum_{i \in \mathcal{V}_w} \rho_i \neq 0$, the system becomes unbalanced, i.e. $\sum_{i \in \mathcal{V}} p_i^{(0)} \neq 0$. If there is no frequency control, the system equilibrates within a few seconds at:

$$\omega = \frac{\sum_{i \in \mathcal{V}_w} \rho_i}{\sum_{k \in \mathcal{V}_g} \gamma_k}, \quad (14)$$

where ω is a deviation from the rate frequency and γ_k is the (natural) damping coefficient of the generator k .

On the other hand, in presence of the primary frequency control based on the affine policy, conventional generators would follow wind power output fluctuations as:

$$\forall i \in \mathcal{V}_g : p_i^{(0)} \rightarrow p_i = p_i^{(0)} - \alpha_i^{(1)} \omega_i. \quad (15)$$

The response of conventional generators given in Eq. (15) would force the system to equilibrate within a few seconds at:

$$\omega^{(1)} = \frac{\sum_{i \in \mathcal{V}_w} \rho_i}{\sum_{i \in \mathcal{V}_g} (\alpha_i^{(1)} + \gamma_i)}, \quad (16)$$

where $\alpha_i^{(1)}$ is the primary droop coefficient (participation factor) of conventional generator i . Following the primary frequency control, the secondary frequency control, also called Automatic Generation Control (AGC) [10], would be deployed within a few minutes, thus adding an additional affine correction to the power output of conventional generators. Thus, Eq. (15) can be modified to account for the secondary frequency control deployment as follows:

$$\forall i \in \mathcal{V}_g : p_i^{(0)} \rightarrow p_i = p_i^{(0)} - \alpha_i^{(1)} \omega^{(1)} - \alpha_i^{(2)} \omega^{(2)}, \quad (17)$$

where $\alpha_i^{(2)}$ is the secondary droop coefficient (participation factor) of conventional generator i . Eq. (17) assumes that the additional correction is distributed among conventional generators according to $\alpha_i^{(2)}$ and ensures that the system is globally balanced after both the primary and secondary frequency responses are fully deployed. Note that Eq. (17) ignores the inter-area correction component to simplify notations. Using Eq. (16) and Eq. (17) leads to the following expression:

$$\omega^{(2)} \sum_{i \in \mathcal{V}_g} \alpha_i^{(2)} = \sum_{i \in \mathcal{V}_w} \rho_i - \omega^{(1)} \sum_{i \in \mathcal{V}_g} \alpha_i^{(1)} = \omega^{(1)} \sum_{i \in \mathcal{V}_g} \gamma_i^{(1)}, \quad (18)$$

It is noteworthy that the secondary control is centralized and, therefore, it is considered as an addition to the local primary control, see [10].

Note that $\omega^{(1)}$ and $\omega^{(2)}$ can each be expressed in terms of $\sum_{i \in \mathcal{V}_w} \rho_i$ using Eq. (18). These expressions can then be combined with Eq. (17) to modify Eq. (4)–(5) as follows:

$$\forall i \in \mathcal{V} : \sum_{j \sim i} \beta_{ij} (\theta_i - \theta_j) = \begin{cases} p_i^{(0)} - \tilde{\alpha}_i \sum_{k \in \mathcal{V}_w} \rho_k, & i \in \mathcal{V}_g \\ \rho_i, & i \in \mathcal{V}_w \\ p_i, & i \in \mathcal{V}_l \end{cases} \quad (19)$$

where $\tilde{\alpha}_i$ stands for the renormalized droop coefficient of conventional generators computed as given below:

$$\forall i \in \mathcal{V}_g : \tilde{\alpha}_i = \frac{\alpha_i^{(1)} + \alpha_i^{(2)} \frac{\sum_{k \in \mathcal{G}_g} \gamma_k^{(1)}}{\sum_{l \in \mathcal{V}_g} \alpha_l^{(2)}}}{\sum_{m \in \mathcal{V}_g} (\alpha_m^{(1)} + \gamma_m^{(1)})}. \quad (20)$$

The renormalized droop coefficients are subject to the following integrality constraint:

$$\sum_{i \in \mathcal{V}_g} \tilde{\alpha}_i = 1. \quad (21)$$

C. Primary Control and Chance Constraints with the Dead Zone

Eq. (17)–(19) assume that the primary control reacts to a frequency deviation of any size. Even though this assumption is applicable for some systems (e.g. microgrids), it does not necessarily hold in relatively large systems, where the primary frequency control is routinely kept untarnished during normal operations and is used to instantly respond to relatively large disturbances, e.g. contingencies. In the latter systems, $\alpha_i^{(1)}$ depends on the size of the frequency deviation, $\omega^{(1)}$, and can be formalized as:

$$\forall i \in \mathcal{V}_g : \alpha_i^{(1)} \rightarrow \alpha_i^{(1)} \begin{cases} 0, & |\omega^{(1)}| \leq \bar{\Omega} \\ 1, & \text{otherwise} \end{cases}, \quad (22)$$

where parameter $\bar{\Omega}$ is a frequency threshold (dead zone) for the primary frequency response, i.e. the range of frequency deviations on the speed-droop governor characteristic that do not trigger the primary frequency response. The value of this threshold can be manually chosen as it suits needs of a particular system, [20]. Note that the dead zone makes the frequency control policy given by Eq. (22) nonlinear; hence, using an affine policy would cause some inaccuracy.

The dead zone introduced by Eq. (22) can be factored in the chance constraints on conventional generators given by Eq. (8)–(9) as follows:

$$\forall i \in \mathcal{V}_g : \mathbb{E}_\rho [\theta(\underline{p}_i - p_i) \theta(\bar{\Omega} - |\omega^{(1)}|)] \leq \varepsilon_i^{(\downarrow, -)}, \quad (23)$$

$$\mathbb{E}_\rho [\theta(\underline{p}_i - p_i) \theta(|\omega^{(1)}| - \bar{\Omega})] \leq \varepsilon_i^{(\downarrow, +)}, \quad (24)$$

$$\mathbb{E}_\rho [\theta(p_i - \bar{p}_i) \theta(\bar{\Omega} - |\omega^{(1)}|)] \leq \varepsilon_i^{(\uparrow, -)}, \quad (25)$$

$$\mathbb{E}_\rho [\theta(p_i - \bar{p}_i) \theta(|\omega^{(1)}| - \bar{\Omega})] \leq \varepsilon_i^{(\uparrow, +)}, \quad (26)$$

where $\theta(x)$ is a step function. This step function is such that $\theta(x) = 1$, if $x > 0$, and $\theta(x) = 0$ otherwise. Eq. (23)–(26)

incorporate both the nonlinear primary frequency response and the wind power generation statistics described by ρ , as given in Eq. (12)-(13). Note that parameters $\varepsilon_i^{(\downarrow,-)}, \varepsilon_i^{(\downarrow,+)}, \varepsilon_i^{(\uparrow,-)}, \varepsilon_i^{(\uparrow,+)}$ are defined similarly to parameters ε_i^\uparrow and ε_i^\downarrow in Eq. (8)-(9).

Section III argues that Eq. (23)–(24) can be represented in a computationally tractable form as one-dimensional integrals with erf-functions. The same transformation can be used for other chance constraints, e.g. Eq. (25)–(26).

D. Weighted CCOPF

Following reference [19], the following weighted chance constraints can be formulated on conventional generators:

$$\forall i \in \mathcal{V}_g :$$

$$\mathbb{E}_\rho \left[\exp \left(-\frac{p_i}{\underline{p}_i} \right) \theta \left(\bar{\Omega} - |\omega^{(1)}| \right) \right] \leq \varepsilon_i^{(\downarrow,-)}, \quad (27)$$

$$\mathbb{E}_\rho \left[\exp \left(-\frac{p_i}{\underline{p}_i} \right) \theta \left(|\omega^{(1)}| - \bar{\Omega} \right) \right] \leq \varepsilon_i^{(\downarrow,+)}, \quad (28)$$

$$\mathbb{E}_\rho \left[\exp \left(\frac{p_i}{\bar{p}_i} \right) \theta \left(\bar{\Omega} - |\omega^{(1)}| \right) \right] \leq \varepsilon_i^{(\uparrow,-)}, \quad (29)$$

$$\mathbb{E}_\rho \left[\exp \left(\frac{p_i}{\bar{p}_i} \right) \theta \left(|\omega^{(1)}| - \bar{\Omega} \right) \right] \leq \varepsilon_i^{(\uparrow,+)}. \quad (30)$$

The advantages of using weighted chance constraints as in Eq. (27)–(30) are three-fold. First, this form makes it possible to prioritize large constraint violations. Second, the convexity of the resulting chance constraints becomes explicit, including for non-Gaussian statistics as shown [19]. Third, there is a computational advantage as the expectations on the left-hand side expressions of Eq. (27)–(30) can be explicitly expressed in terms of the erf-functions.

The final CCOPF-PFR formulation with the weighted chance constraints is as follows:

$$\min_{p_g^{(0)}} \sum_{i \in \mathcal{V}_g} \mathbb{E}_\rho [C_i(p_i)] \quad (31)$$

$$\text{s. t. } \forall i \in \mathcal{V}_g : \text{ Eqs. (27)–(30)} \quad (32)$$

$$\forall \{i, j\} \in \mathcal{E} :$$

$$\mathbb{E}_\rho \left[\exp \left(-\frac{\phi_{ij}}{\underline{\phi}_{ij}} \right) \theta \left(\bar{\Omega} - |\omega^{(1)}| \right) \right] \leq \varepsilon_{ij}^{(\downarrow,-)}, \quad (33)$$

$$(34)$$

$$\mathbb{E}_\rho \left[\exp \left(-\frac{\phi_{ij}}{\underline{\phi}_{ij}} \right) \theta \left(|\omega^{(1)}| - \bar{\Omega} \right) \right] \leq \varepsilon_{ij}^{(\downarrow,+)}, \quad (35)$$

$$(36)$$

$$\mathbb{E}_\rho \left[\exp \left(\frac{\phi_{ij}}{\bar{\phi}_{ij}} \right) \theta \left(\bar{\Omega} - |\omega^{(1)}| \right) \right] \leq \varepsilon_{ij}^{(\uparrow,-)}, \quad (37)$$

$$(38)$$

$$\mathbb{E}_\rho \left[\exp \left(\frac{\phi_{ij}}{\bar{\phi}_{ij}} \right) \theta \left(|\omega^{(1)}| - \bar{\Omega} \right) \right] \leq \varepsilon_{ij}^{(\uparrow,+)}. \quad (39)$$

Note that parameters $\varepsilon_{ij}^{(\downarrow,-)}, \varepsilon_{ij}^{(\downarrow,+)}, \varepsilon_{ij}^{(\uparrow,-)}, \varepsilon_{ij}^{(\uparrow,+)}$ are defined similarly to parameters ε_i^\uparrow and ε_i^\downarrow in Eq. (8)–(9).

III. SOLUTION APPROACH

This section describes how the weighted chance constraints, Eq. (32)–(39), can be computed efficiently. The process is shown for Eq. (27)–(28) and can be extended to other chance constraints. The left-hand side expressions in Eq. (27)–(28) depend on ρ_i and $\bar{\Omega}$ and attain non-zero values if $\bar{\Omega} > |\omega^{(1)}|$ and $\bar{\Omega} < |\omega^{(1)}|$, respectively. Thus, the left-hand-side expressions can be restated as expectations over two distinct Gaussian distributions that can be described by the following means and covariances:

$$\mathbb{E} \left[\omega^{(1)} \right]_\sigma \doteq \Omega_\sigma = \frac{\sum_{i \in \mathcal{V}_w} \bar{\rho}_i}{\sum_{k \in \mathcal{V}_g} (\sigma \alpha_k^{(1)} + \gamma_k)}, \quad (40)$$

$$\begin{aligned} \mathbb{E} \left[(\omega^{(1)} - \Omega_\sigma)^2 \right]_\sigma &\doteq \Theta_\sigma^{(\omega,\omega)} \\ &= \frac{\sum_{i \in \mathcal{V}_w} R_i}{(\sum_{k \in \mathcal{V}_g} (\sigma \alpha_k^{(1)} + \gamma_k))^2}, \end{aligned} \quad (41)$$

$$\forall i \in \mathcal{V}_g : \quad \mathbb{E} [p_i]_\sigma \doteq P_{\sigma;i} = p_i^{(0)} - \tilde{\alpha}_{i;\sigma} \sum_{j \in \mathcal{V}_w} \bar{\rho}_j, \quad (42)$$

$$\begin{aligned} \mathbb{E} \left[(p_i - P_{\sigma;i}) (\omega^{(1)} - \Omega_\sigma) \right]_\sigma &\doteq \Theta_\sigma^{(p_i,\omega)} \\ &= -\frac{\tilde{\alpha}_{i;\sigma} \sum_{j \in \mathcal{V}_w} R_j}{\sum_{k \in \mathcal{V}_g} (\sigma \alpha_k^{(1)} + \gamma_k)} \end{aligned} \quad (43)$$

$$\mathbb{E} \left[(p_i - P_{\sigma;i})^2 \right]_\sigma \doteq \Theta_\sigma^{(p_i,p_i)} = (\tilde{\alpha}_{i;\sigma})^2 \sum_{j \in \mathcal{V}_w} R_j \quad (44)$$

where $\sigma = \{0, 1\}$ distinguish the case “ $\omega^{(1)}$ -in-range” and the case “ $\omega^{(1)}$ -off-range”. If $\sigma = 0$, $\tilde{\alpha}_{i;\sigma} = \tilde{\alpha}_i$. If $\sigma = 1$, $\tilde{\alpha}_i$ is derived from $\tilde{\alpha}_i$ using the replacement $\alpha^{(1)} = 0$. It is also useful to introduce the so-called precision matrices defined as the inverse (2×2) matrices of the covariance matrices

$$\begin{aligned} \forall i \in \mathcal{V}_g : \quad \Phi_{\sigma;i} &= \begin{pmatrix} \Phi_\sigma^{(p_i,p_i)} & \Phi_\sigma^{(p_i,\omega)} \\ \Phi_\sigma^{(p_i,\omega)} & \Phi_\sigma^{(\omega,\omega)} \end{pmatrix} \doteq (\Theta_{\sigma;i})^{-1} \\ &= \frac{\begin{pmatrix} \Theta_\sigma^{(\omega,\omega)} & -\Theta_\sigma^{(p_i,\omega)} \\ -\Theta_\sigma^{(p_i,\omega)} & \Theta_\sigma^{(p_i,p_i)} \end{pmatrix}}{\Theta_\sigma^{(p_i,p_i)} \Theta_\sigma^{(\omega,\omega)} - (\Theta_\sigma^{(p_i,\omega)})^2}. \end{aligned} \quad (45)$$

Next, Eq. (27) can be simplified as:

$$\begin{aligned} &\int_{-\infty}^{+\infty} dx \left(\exp \left(\frac{x}{\underline{p}_i - P_{0;i}} \right) - 1 \right) \times \\ &\int_{-\bar{\Omega} - \Omega_0}^{\bar{\Omega} - \Omega_0} dy \frac{\sqrt{\det(\Phi_{0;i})} \exp \left(-\frac{1}{2} (x, y) \Phi_{0;i} \begin{pmatrix} x \\ y \end{pmatrix} \right)}{2\pi}. \end{aligned} \quad (46)$$

Eq. (46) is convex with respect to set points of conventional generators. Note that the chance constraints in Eq. (28)–(30), (34)–(39) can be converted into similar convex expressions.

IV. CASE STUDY

A. Input Data

The proposed CCOPF-PFR is compared to the standard CCOPF on a modification of the 118-bus Reliability Test System [22]. The test system includes 54 conventional generation resources and 186 transmission lines. Additionally, this system includes 9 wind farms with the total power output forecast of 1,053 MW as itemized in Table I. The mean and standard deviation of the wind power forecast error are set to 0% and 10% of the power forecast at each wind farm. The power flow limit of each transmission line is reduced by 25% of its rated value and the active power demand is increased by 10% at each bus. The droop coefficients (participation factors) of each conventional generator in the CCOPF formulation is set to $1/N_g$, where N_g is the number of conventional generators. The value of the dead zone for the primary frequency response is 100 MW and the likelihood of constraint violations is assumed such that $\varepsilon_i^\downarrow = \varepsilon_i^\uparrow = \varepsilon, \forall i \in \mathcal{V}_g$, and $\varepsilon_{ij}^\uparrow = \varepsilon_{ij}^\downarrow = \varepsilon, \forall \{i, j\} \in \mathcal{E}$. Both the CCOPF and CCOPF-PFR formulations are implemented in Julia [23] using the JumpChance package and solved using a 1.6 Ghz Intel Core i5 processor with 8GB of RAM.

TABLE I. WIND POWER FORECAST AT WIND FARMS ($\bar{\omega}$, MW)

bus #	3	8	11	20	24	38	43	49	50
$\bar{\omega}$	70	147	102	105	113	250	118	76	72

B. Comparison of the CCOPF and CCOPF-PFR solution

First, the CCOPF and CCOPF-PFR formulations are solved for different values of ε . Table II compares the objective functions of these formulations and their CPU times. In general, the CCOPF-PFR consistently yields a more expensive solution. As the value of parameter ε reduces so does the relative difference between the objective function of the CCOPF and CCOPF-PFR formulations. This observation suggests that a nonlinear primary frequency response policy comes at a lower cost for risk-averse OPF solutions. At the same time, the computing times reported in Table II suggest that a higher level of modeling accuracy in the CCOPF-PFR formulation comes at a minimum, if any, increase in computing times.

Second, the CCOPF and CCOPF-PFR solutions presented in Table II are tested against a set of 10,000 random realizations of wind power forecast errors, where each random realization is sampled using the multivariate Gaussian distribution. In each test, the decisions produced by the CCOPF and CCOPF-PFR formulations are fixed and the constraint violations are calculated.

Fig. 1 displays the expected operating cost and its standard deviation observed over 10,000 tests for the CCOPF and CCOPF-PFR formulations. For both formulations the expected operating cost and its standard deviation monotonically change with the value of parameter ε . Thus, the expected operating cost under both formulations gradually

TABLE II. OBJECTIVE FUNCTION VALUES AND CPU TIMES FOR THE CCOPF AND CCOPF-PFR FORMULATIONS

ε	Objective function, \$		CPU time, s	
	CCOPF	CCOPF-PFR	CCOPF	CCOPF-PFR
10^{-1}	91,504.8	94,757.3 (+3.55%)*	10.4	17.3
10^{-2}	92,984.6	94,861.5 (+2.02%)*	11.9	18.1
10^{-3}	94658.7	96,045.3 (+1.46%)*	12.1	19.4
10^{-4}	97,615.1	98,101.4 (+0.49%)*	21.7	18.9

* – the percentage values are relative to the CCOPF formulation.

increases for higher values of parameter ε , while the standard deviation reduces. Notably, in all instances displayed in Fig. 1 the expected cost of the CCOPF-PFR formulation is greater than the expected cost of the CCOPF formulation. As in the cost results presented in Table II, the gap between the expected costs of both formulations reduces for higher values of parameter ε . On the other hand, the CCOPF-PFR formulation leads to a lower standard deviation in all instances, which suggests that the CCOPF-PFR formulation is more cost-efficient for accommodating relatively large wind power forecast errors. A more expensive and conservative CCOPF-PFR solution leads to less violations of chance constraints on conventional generators as shown in Fig. 2. The number of violations reduces for the entire system and for individual generators of different sizes. Therefore, the CCOPF-PFR formulation is more effective in accommodating deviations from the forecast values. Furthermore, there is no noticeable difference in violations of chance constraints on line flows between the CCOPF and CCOPF-PFR formulation. This observation suggests that the CCOPF-PFR mainly improves compliance with operating limits on the supply side.

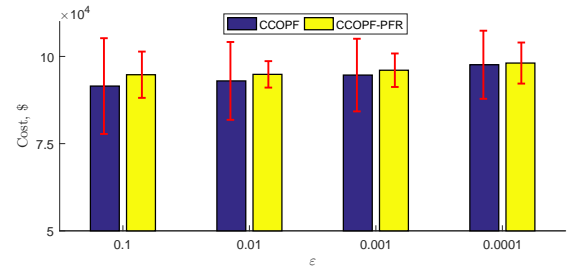


Fig. 1: Comparison of the CCOPF and CCOPF-PFR formulations in terms of the expected costs (vertical bars) and standard deviations (error bars) for different values of parameter ε .

V. CONCLUSION

In this paper, the CCOPF formulation from [11] has been enhanced to explicitly model primary frequency response constraints based on a nonlinear speed-droop governor characteristic of conventional generators. The proposed CCOPF-PFR formulation has been compared to the original CCOPF formulation using a modification of the 118-bus IEEE Reliability Test System [22]. This comparison indicates that modeling a nonlinear speed-droop governor characteristic modestly increases the expected operating cost, while improving adaptability of the dispatch solutions to relative large

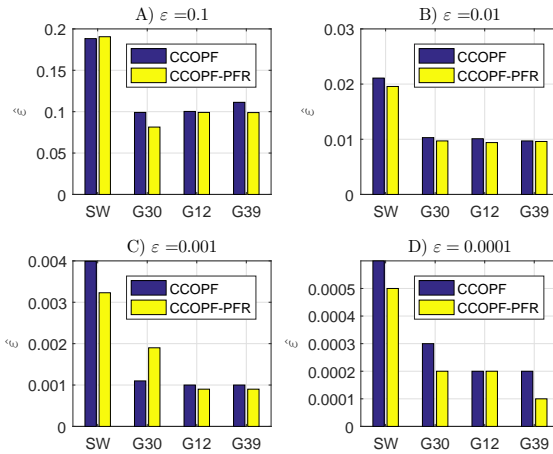


Fig. 2: Empirical violations of chance constraints on conventional generators, $\hat{\epsilon}$, for different values of parameter ϵ . Label SW (system-wide) denotes the fraction of realizations that lead to a violation of at least one chance constraint in the entire transmission system. Labels G30, G12 and G38 denote the fraction of realizations that lead to violations of chance constraints for the maximum power output at conventional generators G30 ($\bar{p}_i = 805.2$ MW), G12 ($\bar{p}_i = 413.9$ MW) and G38 ($\bar{p}_i = 104.0$ MW)

deviations from the forecast. The increased adaptability of the CCOPF-PFR formulation is observed in terms of reduced violations of chance constraints on conventional generators and lower standard deviations of the operating cost. Based on the instances solved in this paper, the proposed CCOPF-PFR and standard CCOPF formulations are comparable in terms of required computational resources.

This work can be extended in several ways:

- Primary frequency control can be generalized to explicitly account for instant power flow fluctuations in transmission lines in proximity of conventional generators in addition to local frequency measurements.
- The proposed CCOPF-PFR model can be enhanced to include an endogenous contingency reserve assessment, e.g. a probabilistic security-constrained framework [24]. The proposed primary frequency response constraints can be used to accurately estimate the minimum response requirement and its allocation instead of using deterministic heuristics, [20].

REFERENCES

- [1] F. Pazheri, M. Othman, and N. Malik, "A review on global renewable electricity scenario," *Renewable and Sustainable Energy Reviews*, vol. 31, pp. 835 – 845, 2014.
- [2] N. Troy, E. Denny, and M. O'Malley, "Base-load cycling on a system with significant wind penetration," *IEEE Trans. Pwr. Syst.*, vol. 25, no. 2, pp. 1088–1097, May 2010.
- [3] J. Eto. Use of a frequency response metric to assess the planning and operating requirements for reliable integration of variable renewable generation. [Online]. Available: <https://www.ferc.gov/industries/electric/indus-act/reliability/frequencyresponsemetrics-report.pdf>
- [4] Y. V. Makarov, C. Loutan, J. Ma, and P. de Mello, "Operational impacts of wind generation on california power systems," *IEEE Trans. Pwr. Syst.*, vol. 24, no. 2, pp. 1039–1050, May 2009.
- [5] Y. Dvorkin, D. S. Kirschen, and M. A. Ortega-Vazquez, "Assessing flexibility requirements in power systems," *IET Generation, Transmission Distribution*, vol. 8, no. 11, pp. 1820–1830, 2014.
- [6] P. Du and Y. Makarov, "Using disturbance data to monitor primary frequency response for power system interconnections," *IEEE Trans. Pwr. Syst.*, vol. 29, no. 3, pp. 1431–1432, May 2014.
- [7] J. W. Ingleson and E. Allen, "Tracking the eastern interconnection frequency governing characteristic," in *IEEE PES General Meeting*, July 2010, pp. 1–6.
- [8] R. Doherty, G. Lalor, and M. O'Malley, "Frequency control in competitive electricity market dispatch," *IEEE Trans. Pwr. Syst.*, vol. 20, no. 3, pp. 1588–1596, Aug 2005.
- [9] J. F. Restrepo and F. D. Galiana, "Unit commitment with primary frequency regulation constraints," *IEEE Trans. Pwr. Syst.*, vol. 20, no. 4, pp. 1836–1842, Nov 2005.
- [10] N. Jaleeli, L. S. VanSlyck, D. N. Ewart, L. H. Fink, and A. G. Hoffmann, "Understanding automatic generation control," pp. 1106–1122, 1992.
- [11] D. Bienstock, M. Chertkov, and S. Harnett, "Chance-constrained optimal power flow: Risk-aware network control under uncertainty," *SIAM Review*, vol. 56, no. 3, pp. 461–495, 2014.
- [12] Y. Yuan, Q. Li, and W. Wang, "Optimal operation strategy of energy storage unit in wind power integration based on stochastic programming," *IET Ren. Pwr. Gen.*, vol. 5, no. 2, pp. 194–201, March 2011.
- [13] R. A. Jabr, "Adjustable robust opf with renewable energy sources," *IEEE Trans. Pwr. Syst.*, vol. 28, no. 4, pp. 4742–4751, Nov 2013.
- [14] Y. Dvorkin, Y. Wang, H. Pandzic, and D. Kirschen, "Comparison of scenario reduction techniques for the stochastic unit commitment," in *2014 IEEE PES Gen. Meet.*, July 2014, pp. 1–5.
- [15] M. Lubin, Y. Dvorkin, and S. Backhaus, "A robust approach to chance constrained optimal power flow with renewable generation," *IEEE Trans. Pwr. Syst.*, vol. 31, no. 5, pp. 3840–3849, Sept 2016.
- [16] Y. Dvorkin, M. Lubin, S. Backhaus, and M. Chertkov, "Uncertainty sets for wind power generation," *IEEE Trans. Pwr. Syst.*, vol. 31, no. 4, pp. 3326–3327, July 2016.
- [17] L. Roald, S. Misra, T. Krause, and G. Andersson, "Corrective control to handle forecast uncertainty: A chance constrained optimal power flow," *IEEE Trans. Pwr. Syst.*, vol. 32, no. 2, pp. 26–37, March 2017.
- [18] L. Roald, G. Andersson, S. Misra, M. Chertkov, and S. Backhaus, "Optimal power flow with wind power control and limited expected risk of overloads," in *2016 Power Systems Computation Conference (PSCC)*, June 2016, pp. 1–7.
- [19] L. Roald, S. Misra, M. Chertkov, and G. Andersson, "Optimal power flow with weighted chance constraints and general policies for generation control," in *2015 54th IEEE Conference on Decision and Control (CDC)*, Dec 2015, pp. 6927–6933.
- [20] Y. Dvorkin, P. Henneaux, D. S. Kirschen, and H. Pandzic, "Optimizing primary response in preventive security-constrained optimal power flow," *IEEE Systems Journal*, vol. PP, no. 99, pp. 1–10, 2016.
- [21] Y. M. Al-Abdullah, M. Abdi-Khorsand, and K. W. Hedman, "The role of out-of-market corrections in day-ahead scheduling," *IEEE Trans. Pwr. Syst.*, vol. 30, no. 4, pp. 1937–1946, July 2015.
- [22] R. D. Christie. Power systems test case archive. [Online]. Available: http://www2.ee.washington.edu/research/pstca/pf118/pg_tca118bus.htm
- [23] M. Lubin and I. Dunning, "Computing in operations research using julia," *INFORMS J. on Comp.*, vol. 27, no. 2, pp. 238–248, 2015.
- [24] R. Fernandez-Blanco, Y. Dvorkin, and M. A. Ortega-Vazquez, "Probabilistic security-constrained unit commitment with generation and transmission contingencies," *IEEE Trans. Pwr. Syst.*, vol. 32, no. 1, pp. 228–239, Jan 2017.